

Visualizing the Atomic Structure Between YSZ and LSM: An Interface Stabilized by Complexions?

T. Götsch,^a H. Türk,^{b,c} F.-P. Schmidt,^{a,d} I. C. Vinke,^e L.G.J. (B.) de Haart,^e R. Schlögl,^{a,d}
K. Reuter,^{b,c} R.-A. Eichel,^{e,f} A. Knop-Gericke,^{a,d} C. Scheurer,^{b,c} T. Lunkenbein^a

^a Fritz-Haber-Institut der Max-Planck-Gesellschaft, Department of Inorganic Chemistry,
14195 Berlin, Germany

^b Fritz-Haber-Institut der Max-Planck-Gesellschaft, Theory Department, 14195 Berlin,
Germany

^c Technische Universität München, Department of Chemistry, Chair of Theoretical
Chemistry and Catalysis Center, 85748 Garching, Germany

^d Max Planck Institute for Chemical Energy Conversion, Department of Heterogeneous
Reactions, 45470 Mülheim an der Ruhr, Germany

^e Forschungszentrum Jülich GmbH, Institute for Energy and Climate Research,
Fundamental Electrochemistry (IEK-9), 52425 Jülich, Germany

^f RWTH Aachen University, Institute of Physical Chemistry, 52056 Aachen, Germany

The YSZ/LSM electrolyte/electrode interface of a half cell is investigated using electron microscopic and theoretical techniques. It is found that, due to strong interdiffusion of all cations except for Sr across the phase boundary, a so-called complexion is formed on the YSZ-side of the interface. This complexion is thermodynamically stabilized by the neighboring bulk phases and its consequences on activity and stability of SOCs are further discussed.

Introduction

Due to their promising role in renewable energy infrastructures, solid oxide cells (SOCs), including fuel and electrolysis cells (SOFCs, SOECs), gain much attention for their high efficiencies (1). As shown in Figure 1 for an SOEC operating under water splitting conditions, these cells consist of two electrodes that are spatially separated by a solid oxide electrolyte, e.g. yttria-stabilized zirconia (YSZ) (2). At the fuel electrode (mostly Ni/YSZ), water is reduced to H₂, whereas the oxygen is conducted as O²⁻ through the electrolyte to the air electrode (lanthanum strontium manganite, LSM), where the oxygen anions are oxidized to molecular O₂ in the oxygen evolution reaction (OER). As schematically shown in the inset for the air electrode side, the actual reaction takes place at the so-called triple phase boundary (TPB), where electrolyte, electrode and gas phase meet: the O²⁻ is delivered by the ion-conducting electrolyte, while the electrons are transported in the purely electron-conducting LSM, and O₂ escapes to the gas phase.

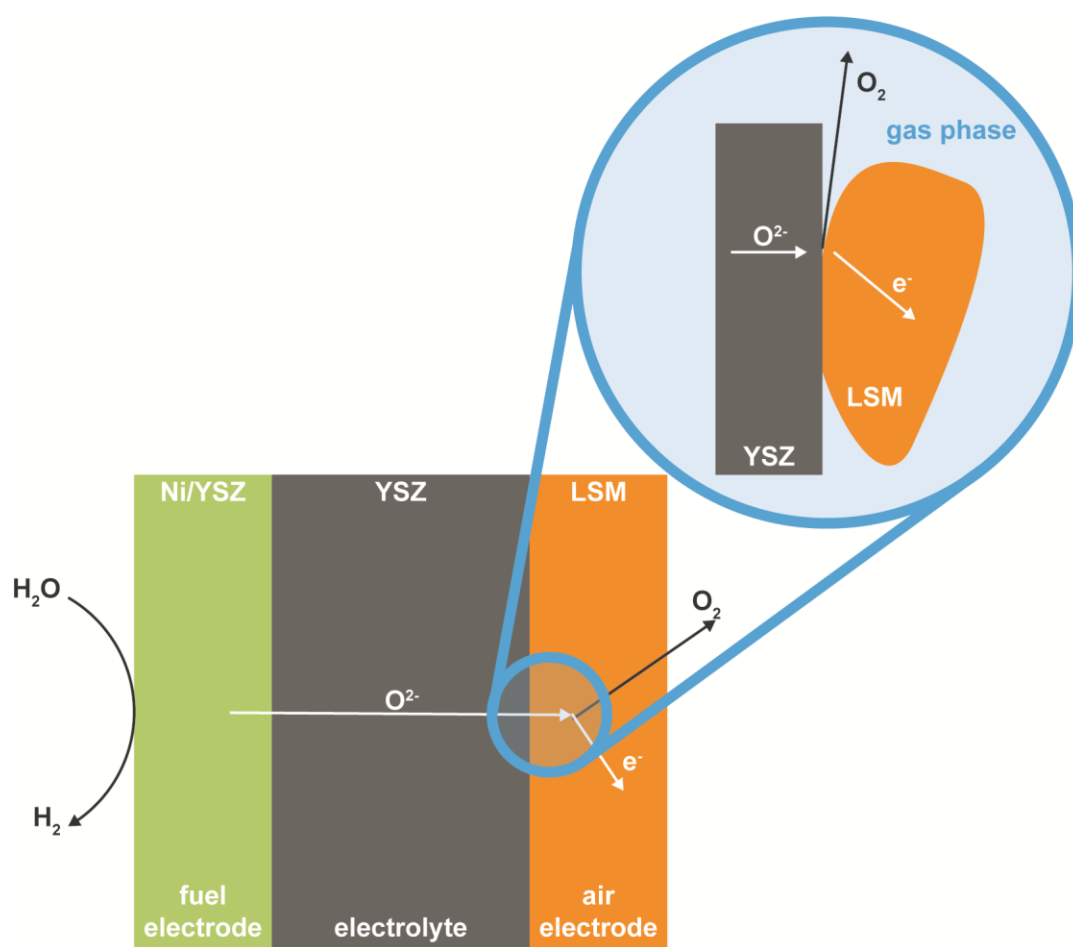


Figure 1. Illustration of SOEC operation with a purely electron-conducting air electrode such as LSM. The oxygen evolution reaction takes place at the interface where electrolyte, electrode and gas phase meet.

Consequently, the interface between electrolyte and electrode forms the underlying foundation for the functionality of these devices. However, studies of the interface are sparse (3)–(6). For instance, it was previously found that the interface between 8YSZ (YSZ with 8 mol% Y_2O_3) and LSM does not form any interlayer while, for 3YSZ, a region of cubic zirconia was observed (3).

In this work, we present a combined experimental and theoretical study that suggests an alternative description of the 8YSZ/LSM interface, namely the formation of a so-called complexion (7) during sintering, and discuss potential implications this complexion might have on the operation of SOCs. A complexion is a thin layer of typically reduced long-range order and self-limited width, which itself is thermodynamically stabilized by the confinement between two bulk regions, yet cannot exist on its own as a bulk phase (8),(9). This complexion layer may have chemical properties that differ severely from the neighboring materials, which possibly influences the activity of SOCs strongly, as will be discussed later.

Experimental

Sample Preparation

Half cells, consisting of 8YSZ || LSM + 8YSZ || LSM, were prepared by screen-printing the electrode layers onto YSZ electrolyte discs (20 mm diameter and 300 μm thickness, Kerafol[®]). An LSM/YSZ (50:50) mixture and pure LSM ($(\text{La}_{0.8}\text{Sr}_{0.2})_{0.95}\text{O}_{3-\delta}$) were consequently deposited with diameters of 8 mm and thicknesses of 25 μm . The cells were sintered in air at 1423 K for 1 h (heating rate: 2 K min^{-1}).

Electron Microscopy

High-resolution scanning transmission electron microscopy (HR-STEM) images were acquired on a double-corrected Jeol JEM-ARM200F operated at 200 kV and equipped with a cold field emission gun.

Energy-dispersive X-ray spectroscopy (EDX) spectrum images were recorded using a ThermoFisher Scientific Talos F200X (200 kV), equipped with four silicon drift detectors in Super-X configuration.

Theoretical Methods

Parallel-tempering Monte Carlo (MC) simulations reaching from 1500–3100 K with cumulatively growing swapping regions centered at the interface were based on force field NPT equilibrations and structure relaxations employing LAMMPS (10). The simulation cells were of a size of 1.56 \times 1.56 \times 18.32 nm and a total of 3731 atoms (2371 O, 320 Mn, 64 Sr, 256 La, 58 Y and 662 Zr) with randomly distributed doping. The interface had an [100] orientation in both cubic materials.

Results

As there is always the risk of introducing artifacts by the preparation of TEM specimens such as a ‘smearing out’ of interfaces due to the different cutting procedures, three different preparation routines were applied to varying locations within the cells in order to exclude preparational artifacts and damages and sample possibly different interface realizations. STEM dark field images are shown in Figure 2a-c, where, in all cases, YSZ is in the lower half of the image (large grains) and LSM is found in the upper half (smaller grains in porous structure). In Figure 2a, the sample was prepared by means of focused ion beam (FIB), exclusively. Using a Ga beam, a trench was dug into the electrode layer to reach the electrolyte/electrode interface, from where a lamella was extracted using standard lift-out techniques. In Figure 2b, on the other hand, a tilted cross-section was prepared by mechanical cutting and polishing, from which a FIB lamella was taken, and in Figure 2c, the sample was cut and thinned only by mechanical methods, without FIB cutting.

In all cases, the sample was oriented in a way to image in a projection parallel to the interface of interest, i.e. to not introduce artificial broadening of the interface by mistilt. The insets in Figure 2a-c show elemental distribution maps of these interfaces with La, Mn and Zr/Y intensities color-coded. The elemental line profiles along the arrows shown in Figure 2a-c are plotted below in Figure 2d-f for all cations present in the system. In all

cases, there is significant inter-diffusion with a diffusion layer of around 1.25 nm width. As there is virtually no difference in the appearance of the elemental distribution profiles between the three specimens, preparational artifacts can be excluded. Another feature that all three elemental profiles share is the fact that the strontium profile is shifted to the LSM side (right-hand side in all plots) by about 0.8 nm, which acts as additional evidence for the lack of preparational damage (otherwise, Sr would have to behave the same way as the other elements).

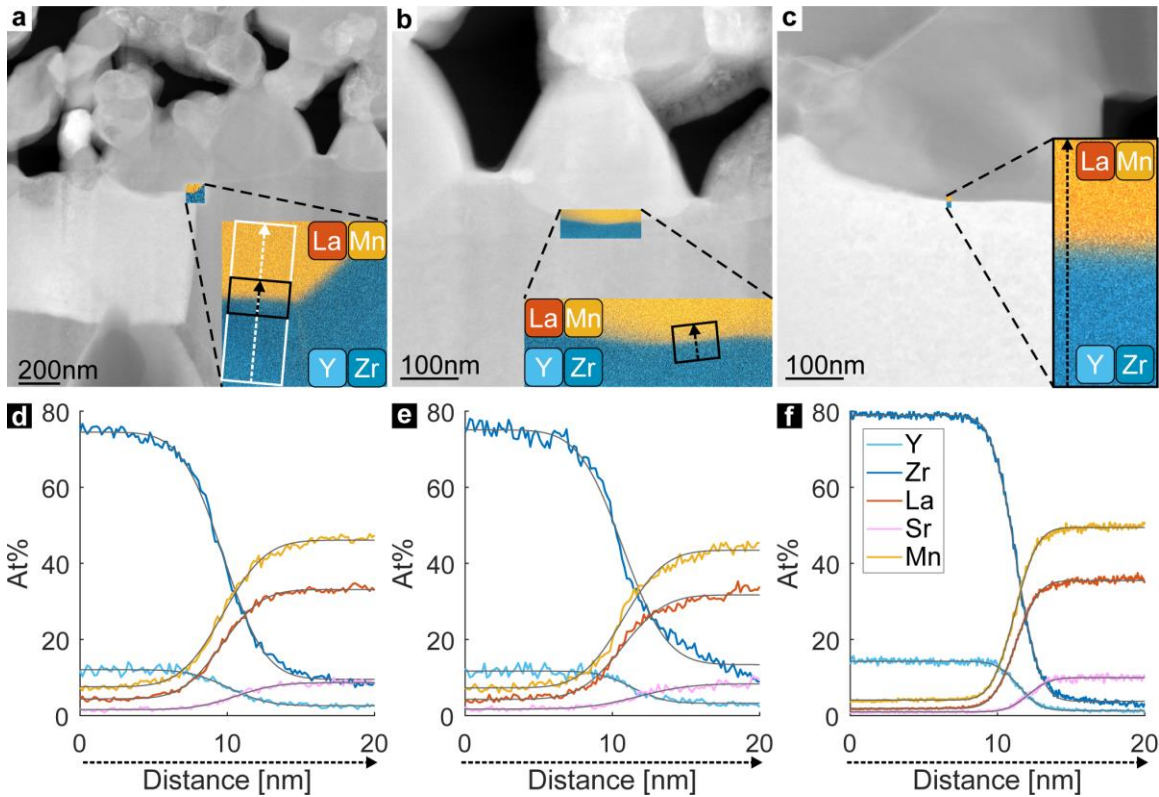


Figure 2. STEM-EDX spectrum images (a-c) and the corresponding elemental profiles (d-f) of the sintered cells show a significant degree of inter-diffusion between YSZ electrolyte and LSM electrode for different sample preparation techniques. Strontium forms an exception in that its elemental profile is shifted with respect to all others – it does not take part in the cross-diffusion.

MC simulations (Figure 3) corroborate these findings: as seen in Figure 3a, all cations, with the exception of Sr that, again, is shifted the same way as observed in the EDX data, interdiffuse (the width of this diffusion region is 1.3 nm compared to 1.25 nm for the experimental data). The atomic arrangement from a snapshot taken at the end of the MC simulation in Figure 3b reveals that, in this interdiffusion layer, which mainly resides on the YSZ side of the interface, there is a noticeable degree of disorder. This becomes clearer in Figure 3c, where a density projection is shown to mimic TEM images, and especially in Figure 3d. In the latter, partial Fast Fourier transforms (FFTs) were computed for thin slabs extracted along the simulation cell. The y axis is thereby shared with the real-space images in Figure 3b,c, whereas the x axis is in Fourier (i.e. reciprocal) space. In the region of the interdiffusion layer, some long-range order reflexes are lost, indicating a slight amorphization in this region.

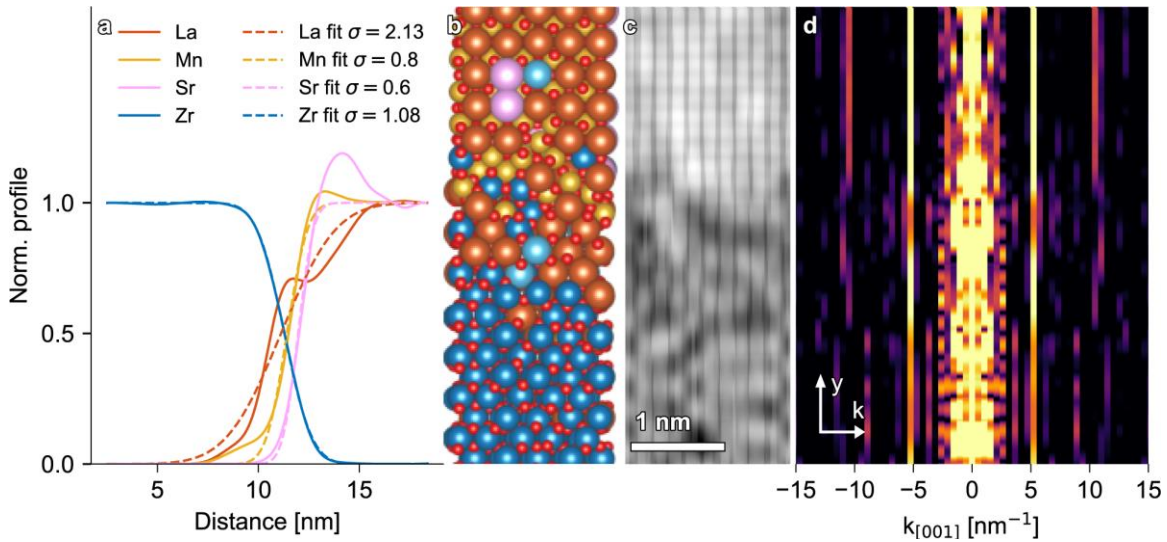


Figure 3. Calculated elemental distribution by Monte Carlo simulations: (a) elemental distribution profiles, also highlighting the shift in the Sr signal. (b) atomic model as obtained by MC, with (c) the corresponding density map and (d) a windowed Fourier transform indicating the reduced order in the complexed region.

This is in line with a phenomenon called complexation, which was originally observed for doped alumina species (8),(9) and describes a layer of reduced order that serves as the transition of two lattice terminations that are in interfacial contact. While, for alumina, external dopants were required to trigger the complexation formation, in the case of the YSZ/LSM interface, the doping is intrinsic and comes from the interdiffusion of the numerous cations as described above. The loss of long-range order was also observed experimentally using high-resolution STEM (not shown here) for the same location as in Figure 2 (7).

The Dillon-Harmer nomenclature distinguishes several types of complexions, depending on the thickness and degree of order (9), such as mono-, bi- or trilayers. Even though the layer thickness is slightly too large, the complexation between YSZ and LSM resembles most a trilayer complexion in its atomic structure.

The presence of such a complexion may have multiple consequences for the activity of SOCs, as highlighted in Figure 4. With a 'pure' YSZ/LSM interface (i.e. no complexion formation), as outlined in the introduction, the reaction can only take place at the TPB. The same is true if the formed complexion is either a pure oxygen anion or electron conductor (not shown explicitly). On the other hand, there is the possibility that the complexion is a mixed ionic and electronic conductor (MIEC, Figure 4b) or a completely deactivating blocking layer with no conduction at all (Figure 4c). In the former case, the activity would be improved significantly as the active site is transformed from the 1-dimensional TPB to a 2D surface (i.e. the complexion/gas interface), similar to using a MIEC electrode. In fact, there are first indications that the complexion between YSZ and LSM has MIEC properties and is still present after prolonged operation (7).

Discussion

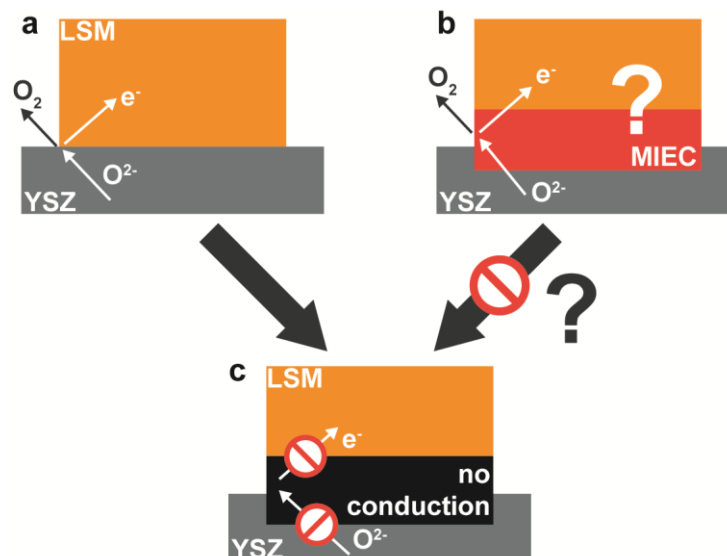


Figure 4. Scheme of possible influences of a complexion on SOCs. a) Without any layer in-between electrolyte and electrode, the reaction takes place at the TPB. b) In case the interlayer is a MIEC, then this would increase the active surface to the whole complexion/gas phase interface, improving performance. c) A non-conducting layer, such as the often-found SrZrO_3 or $\text{La}_2\text{Zr}_2\text{O}_7$, deactivates the cell as no oxygen transport to, nor electron transport from, the active sites is possible anymore. The thermodynamic stability of a complexion potentially inhibits solid state reactions to these deactivating perovskite/pyrochlore layers.

Another point to consider is the thermodynamic stability of the complexion. If a complexion is formed by interdiffusion during sintering, it would effectively inhibit any other solid-state reactions between electrolyte and electrode as long as one stays within the stability regime of the complexion. Consequently, the formation of blocking perovskites (e.g. SrZrO_3) or pyrochlores ($\text{La}_2\text{Zr}_2\text{O}_7$), as are often observed for different electrodes, would not occur. This could explain why LSM is less prone to form pyrochlores than e.g. LSCF ($(\text{La,Sr})(\text{Co,Fe})\text{O}_3$) (11).

Conclusion

We have shown that the YSZ/LSM interface forms a complexion upon sintering, i.e. a thin layer with loss of order that is thermodynamically stable. This is accompanied by strong inter-diffusion of all present cations except for strontium, the elemental distribution of which is shifted to the LSM side by 0.8 nm.

Designing interfaces specifically to obtain complexions with desired properties might be a fruitful route to follow in order to improve performance, i.e. activity and stability of SOCs. If a complexion that is stable under reaction conditions can be formed that, at the same time, exhibits MIEC properties, it would be a significant advancement as both activity and stability could improve strongly.

Acknowledgments

This work was funded by the Deutsche Forschungsgemeinschaft (DFG, German Research Foundation) under the priority programme SPP 2080 DynaKat. T. Götsch additionally acknowledges funding by the Fonds zur Förderung der wissenschaftlichen Forschung (FWF, Austrian Science Fund) via project number J4278. F.-P. Schmidt acknowledges funding by the Deutsche Forschungsgemeinschaft (DFG, German Research Foundation) – 388390466 – TRR 247. This work was further partially funded by the Deutsche Forschungsgemeinschaft (DFG, German Research Foundation) under Germany's Excellence Strategy – EXC 2089/1 – 390776260. The authors thank the Helmholtz-Zentrum Berlin für Materialien und Energie for allocating beam time within proposal number 201-09080CR.

References

1. R. M. Ormerod, *Chem. Soc. Rev.*, **32**, 17–28 (2003).
2. A. Atkinson, S. Barnett, R. J. Gorte, J. T. S. Irvine, A. J. McEvoy, M. Mogensen, S. C. Singhal, and J. Vohs, *Nat. Mater.*, **3**, 17–27 (2004).
3. M. Backhaus-Ricoult, M. Badding, J. Brown, M. Carson, E. Sanford, and Y. Thibault, in *Ceramic Transactions Series*, A. Manthiram, P. N. Kumta, S. K. Sundaram, and S.-W. Chan, Editors, p. 21–30, John Wiley & Sons, Inc., Hoboken, NJ, USA (2012) <http://doi.wiley.com/10.1002/9781118407189.ch3>.
4. M. Brant, T. Matencio, L. Dessemond, and R. Domingues, *Solid State Ion.*, **177**, 915–921 (2006).
5. M. Backhaus-Ricoult, K. Adib, T. St.Clair, B. Luerssen, L. Gregoratti, and A. Barinov, *Solid State Ion.*, **179**, 891–895 (2008).
6. Y. L. Liu, A. Hagen, R. Barfod, M. Chen, H. J. Wang, F. W. Poulsen, and P. V. Hendriksen, *Solid State Ion.*, **180**, 1298–1304 (2009).
7. H. Türk, F.-P. Schmidt, T. Götsch, F. Girgsdies, A. Hammud, D. Ivanov, I. C. Vinke, L. G. J. (Bert) de Haart, R.-A. Eichel, K. Reuter, R. Schlögl, A. Knop-Gericke, C. Scheurer, and T. Lunkenbein, *Mater. Horiz.*, **submitted** (2021).
8. S. J. Dillon, M. Tang, W. C. Carter, and M. P. Harmer, *Acta Mater.*, **55**, 6208–6218 (2007).
9. P. R. Cantwell, M. Tang, S. J. Dillon, J. Luo, G. S. Rohrer, and M. P. Harmer, *Acta Mater.*, **62**, 1–48 (2014).
10. S. Plimpton, *J. Comput. Phys.*, **117**, 1–19 (1995).
11. W. Wang, Y. Huang, S. Jung, J. M. Vohs, and R. J. Gorte, *J. Electrochem. Soc.*, **153**, A2066 (2006).